



current probe. The signal from the quartz sensor was converted using the quartz thickness controller, and was further sent to a PC via a digital data transmission buss RS232. The ion current density was measured using a Faraday-cup single probe. A negative bias potential was applied to the probe to repel the electrons. The sensor signal was converted with an analog-to-digital converter (ADC) and sent to the PC. The vacuum chamber was pumped to a base pressure of  $10^{-3}$  Pa, and Ar was fed into the magnetron gas distribution system. During all the experiments the Ar flow rate was kept constant at the level of 65 sccm, whereas the working pressure in the chamber remained at 0.065 Pa. Discs of Ti (99.9 % purity), Al (99.96 % purity) and Cu (99.9 % purity)  $\ddagger$  80 and 5.0 mm in thickness were used as the magnetron targets. The DC power supply having 1300 W at the maximal power output was employed to supply power for the magnetron. The magnetron discharge current  $I_t$  ranged from 0 up to 4.0 A. The discharge current stabilization mode was used for all the experiments. In order to alter the extent of unbalance the additional coil current  $I_c$  was varied from  $-0.2$  to  $0.5$  A. During the experiments the probes were placed at the distance of 115 mm from the target surface.

### 3 RESULTS AND DISCUSSION

In the series of DC magnetron sputtering of Al, Ti, and Cu targets it was studied how the process parameters and the extent of magnetron's unbalance affect the deposition rate distribution profiles. As different metals were sputtered, it was established that the deposition rate varied almost proportionally to the magnetron's discharge current (Fig. 2). Normalization of the deposition rate profiles, obtained at various discharge currents, proved practically complete coincidence of the profiles describing a certain material. However, the deposition rate profiles demonstrated dependence on the type of the sputtered materials. Evidently, that can be accounted for unequal angular distribution of sputtered particles when various materials are being sputtered [6]. As the additional coil current (unbalance level) increased, negligible changes were observed in the profiles, and the deposi-

tion rate at the magnetron's axis was noticed to drop at constant discharge current (Fig. 3). That process can be associated with a transformation of the sputtering area caused a changing balance of magnetic flows from the outer and central magnetic cores. When the working pressure was varied from 0.04–1.20 Pa the deposition rate for all the studied materials remained almost unchanged. That evidenced the absence of considerable thermalization at given range of pressures.

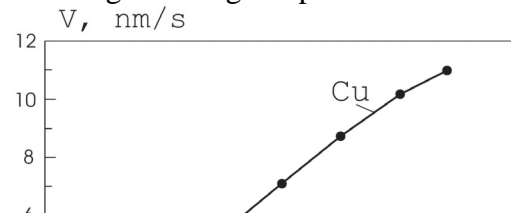


Fig. 2: Magnetron axis deposition rate as a function of discharge current for various types of materials

Fig. 3: Magnetron axis deposition rate as a function of the additional coil current for various types of materials ( $I_t = 2.0$  A)

For the same target materials, the ion current density distributions were obtained as functions of the sputtering process parameters and the extent of magnetron's unbalance. It was established that for all the target materials under study the ion current density at the magnetron's axis grew proportionally to the discharge current and the coil current. As various target materials were being sputtered, the comparison of the ion currents proved that the ion current density was determined by the type

of the sputtered materials. For instance, in case of the Cu target the ion current density at the magnetron's axis reached  $2.5 \text{ mA/cm}^2$ , and under the same conditions increased more than 2 times the ion current of Ti or Al targets (Fig. 4). If the additional coil current (unbalance level) grew the ion flow focusing was observed (Fig. 5). At the same time the ion current density at the edges of the discharge area remained practically at the same level.

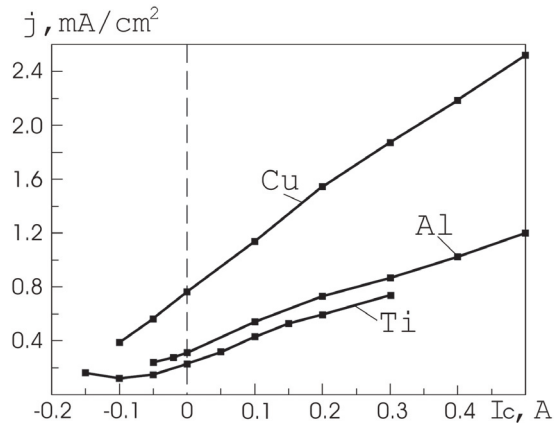


Fig. 4: Ion current density on the magnetron axis as a function of additional coil current for various type of materials ( $I_t = 2.0 \text{ A}$ )

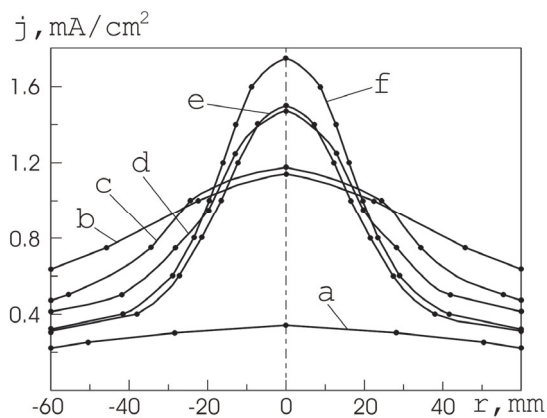


Fig. 5: Distribution of the substrate ion current at magnetron sputtering of Cu target for various additional coil currents

Based on the experimental data obtained, the distribution profiles for the ion-to-atom ratio on the condensing surface were calculated for various deposition conditions. It was proved that in case of DC magnetron sputtering the ion-to-atom ratio on the condensing surface increased if the sputtering yield of the target material dropped down (Fig. 6). When the additional coil current was negative  $-0.1 \text{ A}$  (I-type unbalance) the ion-to-atom ratio for all the sputtering conditions and materials under

study did not exceed 0.15 and had the most uniform distribution. That behavior resulted from the electron flow deviating from the substrate area in a form of a radiating magnetic field, bringing about low-density plasma in the substrate area.

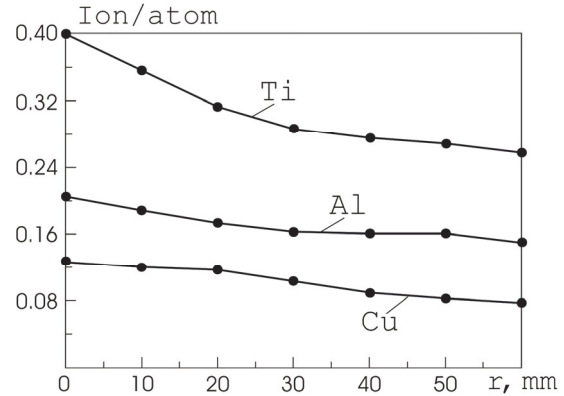


Fig. 6: Ion-to-atom ratio distribution on the condensing surface for various types of materials

#### 4 CONCLUSION

The study of the deposition rate and ion current density profiles at DC magnetron sputtering have shown that the deposition rate varies proportionally to the discharge current and practically does not depend on the unbalance level of the magnetron, whereas the ion current density is determined both by the discharge current and the unbalance level of the magnetron. At the same time the ion-to-atom ratio at the condensing surface is increased when the sputtering yield of the target material goes down. The minimal energy impact on the growing film and the most uniform distribution profile of the ion-to-atom ratio is achieved in the case of I-type unbalance. This MSS operation mode can be used to deposit transparent conducting oxide, superconductor, and ferroelectric thin films.

#### REFERENCES

- [1] Kelly P J, Arnell R D, Vacuum 56 (2000) 159-172.
- [2] Kester D J, Messier R, J Mater Res. 8 (1993) 1938-1957.
- [3] Colligon J S, J Vac Sci Technol A 3 (1995) 1649-1657.
- [4] Svadkovski I V, Golosov D A, Zavatskiy S M, Vacuum 68 (2003) 283-290.
- [5] Golosov D A, Svadkovskii I V, Zavatskii S M Surf Eng Appl Electrochem 6 (2002) 56-64.
- [6] Ekpe S D, Dew S K, J Vac Sci Technol A 21 (2003) 476-483.